American Mineralogist, Volume 63, pages 499–505, 1978

Chevkinite and perrierite from the Oslo region, Norway

TOM VICTOR SEGALSTAD AND ALF OLAV LARSEN

Institutt for Geologi, Universitetet i Oslo
P. O. Box 1047 Blindern, Oslo 3, Norway

Abstract

Chevkinite has been found in three localities of syenite pegmatite in the Oslo region, one of which also carries perrierite. The perrierite and chevkinite do not coexist. The perrierite contains a loparite (with pyrophanite) core. The unheated chevkinites and perrierite gave no X-ray diffraction patterns, due to their metamict state. All chevkinites show well-developed chevkinite X-ray patterns when heated in air, but in the sample with Ce > La the chevkinite pattern is weak and a strong CeO_2 pattern is also present. Unit-cell dimensions correspond with cell parameters given in the literature. The chemical compositions of the chevkinites and perrierite investigated were found to be relatively uniform and suited the formula $A_4BC_4Si_4O_{22}$ where A = REE,Th,Ca,Sr,Na,K; B = Fe^{2+},Mg,Mn,Ca; C = Ti,Mg,Mn,Fe^{2+},Fe^{3+},Al. Phase boundaries for the structural transformations between natural chevkinites and perrierites are given as a function of the average size of the ions occupying the several structural sites. The results of the study tend to confirm that the phase change chevkinite–perrierite is controlled primarily by composition, in that the size of the B and C cations exerts a strong control over the structure. In the chevkinite structure very large cations can therefore only be accomodated in the A positions either by increasing the average size of the B and C cations to open up the structure or by distorting it to give perrierite symmetry.

Introduction

The rare-earth iron titanosilicate chevkinite was first reported by Rose in 1839 from the Urals (Vlasov, 1966); the chemically very similar mineral perrierite was first reported by Bonatti and Gottardi (1950) from Italy. Both minerals have since been found in a variety of localities, usually in pegmatites, but also in igneous rocks and in volcanic ash. To the best of our knowledge the two have never been found to coexist. Good analytical data on these minerals are scarce.

Jaffe *et al.* (1956) suggested that the two names referred to one and the same mineral, but later work (see Gottardi, 1960; Bonatti and Gottardi, 1966), culminating in the structure determinations of Calvo and Faggiani (1974), has established that they have different but very similar structures and virtually identical formulae. The mutual substitution of cations is extensive and several variations of the formula have been suggested. The work of Ito and Arem (1971) resulted in the formula: $A_4B\ C(1)_2\ C(2)_2Si_4O_{22}$ where A = REE,Th,Ca,Sr,Na,K in 10-fold coordination; B = Fe^{2+},Mg,Mn,Ca in 6-fold coordination; C = Ti,Mg,Mn,Fe^{3+},Fe^{2+},Al in 6-fold coordination. Calvo and Faggiani (1974) stated that 9-fold coordination occurs in the A position. In natural chevkinites and perrierites titanium predominates in the C positions [particularly $C(2)$], Fe^{2+} predominates in the B positions, and the larger rare earths (primarily La and Ce) predominate in the A positions.

The two minerals have such similar compositions that they appear to be polymorphs. However, Ito (1967) synthesized chevkinite and perrierite and found that the size of the cations occupying the A, B, and C sites determines which structure will form. He concluded therefore that the two minerals are not polymorphs in the strict sense. Later, however, new synthetic work (Ito and Arem, 1971) demonstrated that certain compositions (*e.g.* $Pr_4Mg_2Ti_3Si_4O_{22}$ and $Pr_4Ni_2Ti_3Si_4O_{22}$) can exist in two structural states. They concluded therefore that dimorphism occurs, but only within fairly narrow chemical limits, and that perrierite transforms to chevkinite with increasing temperature.

Lima-de-Faria (1962), working with natural minerals, observed the opposite effect, namely that of chevkinite converting to perrierite (and exsolving

0003-004X/78/0506-0499$02.00

CeO_2) on heating in air. The same result was recorded by Mitchell (1966) on chevkinite from Virginia. Calvo and Faggiani (1974) stated that their detailed structural studies did not elucidate the role of various ionic radii in the perrierite–chevkinite transformation.

The object of the present study is to record three new localities for these relatively rare minerals (in syenite pegmatites from the southwestern Oslo region, Norway); to provide good analytical data of these minerals (only a few samples from the known localities are well analyzed); and to attempt to use these data to further our understanding of perrierite–chevkinite transformation and stability fields. This is the first reported occurrence of chevkinite in Norway. Perrierite has been reported previously from a quartz-rich pegmatite lens in anorthosite from Sogndal, south Norway (Raade, 1970). It is particularly interesting that, at one of the localities described here, chevkinite and perrierite occur in the same pegmatite but they do not coexist. This means a very close genetic association, although the field relations indicate different periods of crystallization, and thus certain differences in chemistry and temperature or both, in their respective environments of formation.

Occurrence

The rare mineral parageneses in the syenite pegmatites associated with the Permian larvikite (monzonite) of the Oslo region were made famous by the work of Brøgger (1890). The occurrences reported by us are of two main types: one in pegmatites located in basaltic rocks near the contact with larvikite (Bjørkedalen, Stokkøya), the other in pegmatites in massive larvikite (Sandefjord), see Figure 1.

The Bjørkedalen deposit, recently described by Segalstad and Larsen (1978), is the only one where both chevkinite and perrierite occur. Although the mineralogy of the syenite pegmatite material found on the dumps of a water tunnel is variable, aegirine and microcline are always the dominant minerals. Chevkinite occurs in minor amounts as small crystals (up to 3 mm long) in a gadolinite-(Ce)-bearing pegmatite. Perrierite is common in syenite pegmatites where zircon and pyrochlore are also abundant; it occurs in crystal aggregates (single crystals are up to 7 mm long) with a loparite (and pyrophanite) core (Fig. 2). Chevkinite is common as crystals (up to 10 mm long) in deformed syenite pegmatites with abundant zircon, pyrochlore, and magnetite. This paragenesis is very similar to that described by Segalstad and Larsen (1978).

The Stokkøya pegmatite has been described by Brøgger (1890). The chevkinite was found in 1975 as 2–3 cm long crystals in syenite pegmatite veins in basaltic rocks. The 0.5–1.0 m thick pegmatite consists mainly of microcline, biotite, and aegirine. Accessories include zircon, pyrochlore, leucophanite, and pyrophanite. The dike is in places heavily zeolitized with analcite, natrolite, and thomsonite.

Chevkinite from a syenite pegmatite in larvikite at Bugården, Sandefjord, has recently been reported by Ragnar Hansen (personal communication, 1976). It occurs as irregular masses (up to 10 mm in diameter) with microcline, barkevikite, aegirine, magnetite, zircon, and pyrochlore. Apatite is found as cores and inclusions in chevkinite, aegirine, and barkevikite. Ito and Arem (1971) and Izett and Wilcox (1968) also reported apatite as inclusions in chevkinite and perrierite. In contrast to the chevkinites from the previously described occurrences, the mineral here has a 2 mm alteration rim of bastnaesite. This has also been observed on perrierite from Virginia (Mitchell, 1966).

Chevkinites and perrierites from the Oslo region are black and vitreous, and show conchoidal fracture. Density determined using a Berman balance and toluene gave values from 4.46 to 4.67 g/cm^3 for chevkinites and 4.29 g/cm^3 for perrierite (see Table 2). In thin section the minerals are dark reddish-brown and show strong pleochroism.

X-ray crystallography

Unheated chevkinites and perrierite from the Oslo region gave no X-ray diffraction patterns due to their metamict state. To obtain X-ray diffraction patterns the minerals were heated both in air and in nitrogen at 1000°C for one hour according to the method of Lima-de-Faria (1962, 1964). X-ray films were made using a 9 cm Debye-Scherrer camera, and compared with films of the Nettuno perrierite (Bonatti and Gottardi, 1950) and the New Hampshire chevkinite (Jaffe *et al.*, 1956). Sample C (Table 1 and 2) gave a perrierite pattern when heated both in air and in nitrogen. Samples A and D (Table 1 and 2) gave chevkinite patterns when heated both in air and nitrogen. Sample B (Table 1 and 2) gave a good quality chevkinite pattern when heated in nitrogen, but strong CeO_2 lines plus a weak chevkinite pattern when heated in air. This seems to be because Ce is in excess of La in this sample (see Table 2).

d values and cell dimensions for the chevkinites and perrierite heated in nitrogen have been calculated from X-ray powder diffraction films taken with a Guinier quadruple-focussing camera using Fe-radia-

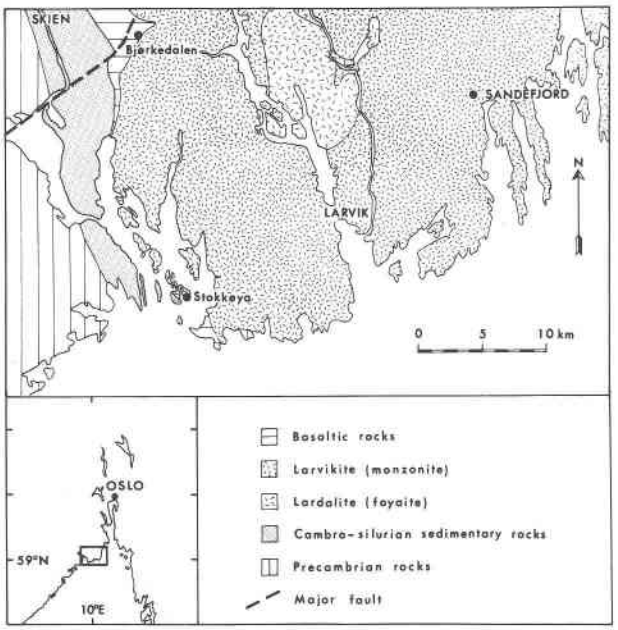

Fig. 1. Sketch map of the bedrock geology of the southwestern Oslo region; dots show the occurrences described in the text.

tion, a quartz monochromator, and lead nitrate as internal standard. The cell dimensions for the chevkinites and perrierite from the Oslo region are given in Table 1. They correspond with cell parameters for chevkinites and perrierites, respectively, given by Ito (1967).

Chemical composition

Electron microprobe analyses on polished sections were made on an ARL-EMX microprobe at the Central Institute of Industrial Research, Oslo, using a series of natural and synthetic standards. Matrix corrections were made according to the method of Bence and Albee (1968), using correction factors from Albee and Ray (1970) and Åmli and Griffin (1975). The rare-earth elements were analyzed by the procedure described by Åmli and Griffin (1975) using the same standards and thus achieving the same accuracy as in their work. Each analysis represents the mean of four analyzed points. The analytical results are presented in Table 2. No zoning was observed in the minerals analyzed. Wet-chemical analysis showed that iron is almost exclusively present as FeO. The structural formulae given in Table 2 were obtained by assigning cations (calculated on the basis of 13 cations per formula unit) to the various structural positions without distinguishing between *C(1)* and *C(2)* sites. The sum of the anions is in every case reasonably close to the ideal value of 22.

Discussion

On first inspection there are close chemical and crystallographical similarities both between the chevkinite and perrierite of the present study and between these data and available analyses of these minerals from other localities (Jaffe *et al.*, 1956; Vlasov, 1966; Mitchell, 1966). It is difficult to discuss observed chemical variations in our samples in terms of the general chemistry of the environment because: (a) the trace-element distribution in the larvikite/lardalite massif is not well known, and (b) a direct genetic relationship between the pegmatite dikes and the larvikite is not known, although there are reasons to believe so (Segalstad and Larsen, 1978). However, the thorium content of these minerals varies sympathetically with the Th values for the larvikite, being high in the Stokkøya area and low at Bjørkedalen (Raade, 1973). The relatively high Sr contents of the perrierite is conspicuous, although still lower than that of the strontian perrierite (with 7.73 weight percent SrO) reported from Baikal, U.S.S.R., by Portnov (1964).

Ito (1967), in his synthetic studies of these phases, plotted the effective size of the cations in the *A* position versus the average effective size of the cations in the *B* and *C* positions, and showed that the structure changed from chevkinite to perrierite when the difference in these two values is excessive. Figure 3 is a plot of this kind using only synthetic materials of the type $A_4BC_4Si_4O_{22}$ which can be restated as

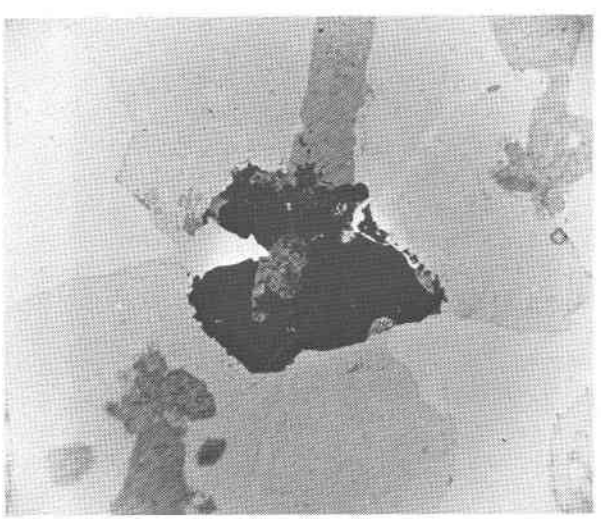

Fig. 2. Photomicrograph showing perrierite (black) from Bjørkedalen, with core of loparite (grey) and pyrophanite (dark grey). The perrierite is surrounded by aegirine (grey) and microcline (light grey). (White areas are the thin section cementing material.) Length of picture 18 mm.

Table 1. Observed and calculated (least squares refinements) *d* values and cell constants for chevkinites and perrierites

CHEVKINITES												PERRIERITES					
	NH		A			B			D				N		C		
hkl	*d*(obs)	*I*	*d*(calc)	*d*(obs)	*I*	*d*(calc)	*d*(obs)	*I*	*d*(calc)	*d*(obs)	*I*	hkl	*d*(obs)	*I*	*d*(calc)	*d*(obs)	*I*
002	5.44	20	5.44	5.44	w	5.43	5.44	w	5.45	5.43	w	002	5.34	65	5.41	5.40	vw
11$\bar{1}$	4.86	40	4.88	4.88	w	4.88	4.88	w	4.87	4.86	w	110	5.13	25	5.16	5.16	w
111	4.60	40	4.61	4.61	w	4.60	4.61	w	4.60	4.60	w	11$\bar{1}$	4.06	20	4.99	5.00	w
003	3.63	5	3.63	3.64	w	3.62	3.55	w	3.63	3.63	w	11$\bar{2}$			4.09	4.09	w
310			3.49	3.49	w	3.49	3.49	w	3.49	3.49	w	003	3.56	20	3.61	3.61	w
												31$\bar{1}$	3.53	15			
31$\bar{1}$	3.47	20	3.48	3.48	w	3.48	3.48	w	3.47	3.48	w	112			3.46	3.47	w
311	3.20	100	3.19	3.20	m	3.19	3.20	m	3.19	3.19	m	40$\bar{1}$	3.43	20	3.40	3.39	vw
11$\bar{3}$			3.10	3.09	w	3.09	3.09	w	3.10	3.10	w	400	3.15	15	3.13	3.14	w
401			3.01	3.01	w	3.01	3.01	w	3.01	3.01	w	40$\bar{3}$	3.03	20	3.05	3.05	w
402	3.08	40										31$\bar{3}$	2.96	100	2.99	2.99	s
												311	2.93	55	2.95	2.96	s
400	3.00	20										020	2.82	65	2.83	2.85	m
113			2.89	2.88	m	2.88	2.88	m	2.89	2.89	m	113			2.75	2.75	w
020	2.86	70										021	2.73	15			
312	2.76	20	2.76	2.77	w	2.76	2.77	w	2.76	2.76	w	004	2.675	20	2.71	2.70	m
004	2.71	100	2.72	2.73	s	2.71	2.73	s	2.73	2.73	s	40$\bar{4}$			2.64	2.64	vw
												220	2.550	15	2.58	2.58	vw
220	2.61	5										312			2.51	2.52	w
022	2.53	20	2.54	2.54	w	2.54	2.54	w	2.54	2.54	w	022	2.488	15	2.51	2.50	vw
222	2.44	5										51$\bar{2}$			2.46	2.47	vw
404	2.32	5										114			2.25	2.25	vw
023	2.24	5	2.25	2.25	vw	2.25	2.24	vw	2.25	2.25	vw	60$\bar{2}$	2.229	50			
												42$\bar{1}$	2.166	25			
42$\bar{1}$			2.18	2.18	m	2.17	2.17	m	2.17	2.16	m	42$\bar{2}$	2.156	25	2.17	2.18	w
421	2.17	70										313			2.14	2.14	vw
42$\bar{2}$	2.08	5	2.10	2.10	w	2.10	2.10	w	2.10	2.10	w	420			2.10	2.08	vw
601			2.08	2.08	vw	2.08	2.08	vw	2.08	2.08	vw	60$\bar{4}$	2.095	15			
314			2.01	2.01	w	2.01	2.01	w	2.01	2.01	w	600	2.088	15			
31$\bar{5}$			1.98	1.98	w	1.98	1.98	w	1.98	1.98	w	024	1.941	50	1.96	1.96	w
	a 13.44		*a* 13.43(2)			*a* 13.44(4)			*a* 13.40(2)				*a* 13.61		*a* 13.70(3)		
	b 5.72		*b* 5.74(1)			*b* 5.73(2)			*b* 5.72(1)				*b* 5.62		*b* 5.66(2)		
	c 11.10		*c* 11.07(1)			*c* 11.04(3)			*c* 11.09(1)				*c* 11.63		*c* 11.83(3)		
	β 100.20		β 100.58(12)			β 100.61(25)			β 100.53(12)				β 113.47		β 113.79(18)		

*The four Oslo region samples (*A, B, C, D*) are heated in nitrogen at 1000° C for 1 hour.* A = *Chevkinite, Stokkøya.* B = *Chevkinite, Sandefjord.* C = *Perrierite, Bjørkedalen.* D = *Chevkinite, Bjørkedalen.* NH = *Heated chevkinite, New Hampshire (data from Ito, 1967).* N = *Unheated perrierite, Nettuno (data from Bonatti, 1959).*
s = *strong.* m = *medium strong.* w = *weak.* vw = *very weak.*
Parenthesized figures represent the estimated standard deviation (esd) in terms of least units cited for the value to their immediate left, thus 100.58(12) indicates an esd of 0.12.

$X_4Y[(Y_1Ti_1)Ti_2]Si_4O_{22}$, where X = a lanthanide element and Y = a transition element. The data of Shannon and Prewitt (1969) for cationic radii in 6-fold coordination have been used in this plot. Nine-fold (Calvo and Faggiani, 1974) coordination radii should have been used for the vertical axis, but these are incomplete and much less reliable than the 6-fold coordination data. Ito's (1967) synthetic phases were prepared over a range of temperatures from 680° to 1400°C, but nevertheless the phase boundary in the graph is defined by a fairly narrow zone in which both phases have been synthesized (indicating that the compositional control is stronger than the temperature effect). Within this zone higher temperatures appear to stabilize the chevkinite structure (Ito, 1967).

Ito pointed out that the reverse transformation, observed on heating naturally-occurring materials in air, can also be interpreted in terms of this diagram. A change in the X-ray diffraction pattern from chevkinite to perrierite is always accompanied by exsolution of CeO_2. The Ce^{3+} which occupied *A* positions in the original chevkinite is oxidized on heating to Ce^{4+}. The latter is too small to occupy the same positions in perrierite and is therefore expelled as CeO_2. Because the other main occupant of *A* positions in naturally-occurring materials is the larger La cation, expulsion of the Ce results in an *increase* in the average size of the cation in *A*. Fe^{2+} is also reduced in size when it is oxidized to Fe^{3+}, but (provided charge-balance requirements permit) it still remains in the same octahedral sites. For a chevkinite composition close to the phase boundary, oxidation will thus shift the composition at right angles to the phase boundary; this may be sufficient to shift the composition into the perrierite field (Fig. 3).

Table 2. Chemical composition (weight percent oxides), structural formulas on the basis of 13 cations, and measured densities (g/cm³) of chevkinites and perrierite from the Oslo region

	A				B				C				D			
	Chevkinite, Stokkøya				Chevkinite, Sandefjord				Perrierite, Bjørkedalen				Chevkinite, Bjørkedalen			
SiO_2	19.49	3.992		4.00	19.18	3.973		4.00	20.64	4.022		4.02	19.86	3.975		4.00
Al_2O_3	0.10	0.024	0.008		tr				0.38	0.088			0.07	0.017		
TiO_2	16.98	2.616	0.016		16.23	2.529	0.027		19.15	2.807			17.07	2.569	0.008	
FeO*	9.13	1.565			10.80	1.870	2.502		8.17	1.331		4.98	10.06	1.683	2.561	
MnO	2.65	0.460		5.00	0.82	0.144		5.00	1.70	0.281			1.01	0.171		5.00
MgO	0.09	0.027			0.13	0.040			0.40	0.116			0.49	0.147		
CaO	2.09	0.459	0.326		2.59	0.575	0.444		3.94	0.823	0.355		3.20	0.686	0.438	
SrO	0.28	0.034	0.133		nd		0.131		1.28	0.145	0.468		0.32	0.037	0.248	
Na_2O	0.14	0.058			0.09	0.037			0.47	0.178			0.17	0.065		
K_2O	0.08	0.020			0.07	0.018			tr				0.07	0.017		
ThO_2	3.55	0.169			3.05	0.143			0.68	0.030			1.62	0.074		
Y_2O_3	0.06	0.007			0.37	0.041			0.40	0.042			0.29	0.031		
La_2O_3	23.75	1.832			19.48	1.489			21.01	1.511			23.76	1.754		
Ce_2O_3	19.63	1.503			22.31	1.692			18.24	1.302			19.26	1.411		
Pr_2O_3	2.36	0.180			2.43	0.183			2.16	0.153			2.46	0.180		
Nd_2O_3	1.52	0.114			3.14	0.232			2.25	0.157			2.32	0.166		
Sm_2O_3	nd			4.08	nd			4.00	nd			4.00	nd			4.00
Eu_2O_3	nd				0.07	0.005			nd				nd			
Gd_2O_3	nd				nd				nd				nd			
Tb_2O_3	0.17	0.012			0.21	0.014			0.13	0.009			0.16	0.015		
Dy_2O_3	0.15	0.010			nd				nd				nd			
Ho_2O_3	0.06	0.004			0.09	0.006			tr				tr			
Er_2O_3	nd				nd				nd				nd			
Tm_2O_3	nd				nd				nd				nd			
Yb_2O_3	0.06	0.004			0.13	0.009			0.11	0.006			0.06	0.004		
Lu_2O_3	nd				nd				nd				nd			
Sum	102.35				101.19				101.10				102.26			
ρ (meas)	4.67				4.63				4.29				4.46			

Traces: U. Not detected: Sc, Nb, Ta, Zr, Hf.

* *Total iron.* tr = *traces.* nd = *not detected.*

Naturally-occurring chevkinite and perrierite differ from the synthetic phases plotted in Figure 3 because of their greater variety of ionic substitutions. In particular, they commonly show considerably less than 3 atoms of Ti per formula unit, because part of the Ti site is occupied by Al and Fe. There are few synthetic data to indicate what effect this may have on the position of the phase boundary of Ito's plot. Figure 4 is a plot of the analyses of eight naturally-occurring materials taken from the literature (Kauffman and Jaffe, 1946; Jaffe *et al.*, 1956; Vlasov, 1966) and our four new analyses, all recalculated on the basis of 13 cations.

In the eight previously-reported analyses Ti + Al occupy at least 3 of the 5 (B + C) positions; the remainder is filled by Fe and Mg. These analyses are chemically so similar that one would expect that the plot used by Ito would provide a clear-cut phase boundary (although one which would not necessarily coincide with that obtained from synthetic studies). Two of the chevkinites (from Madagascar and the Il'menskie Mts.) must lie close to the phase boundary, because they convert to perrierite on heating. If the boundary is drawn through these two points the line separates chevkinites from perrierites, and the position of the line corresponds exactly with the boundary zone defined by Ito's synthetic work.

Our four analyses from the Oslo region are very low in Al compared with previous analyses. This means that most of the Ca present must be assigned

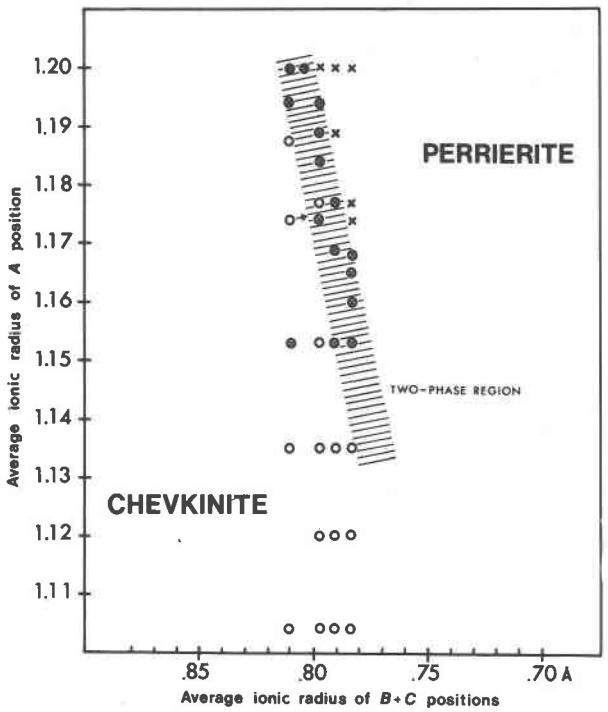

Fig. 3. Distribution of synthetic perrierites and chevkinites (Ito, 1967) as a function of the average ionic radii of the *A* and *B* + *C* positions. Circles: chevkinites; crosses: perrierites; circled crosses: both phases. Arrow: oxidation of a chevkinite containing Ce and Fe will cause a compositional shift towards or into the perrierite field.

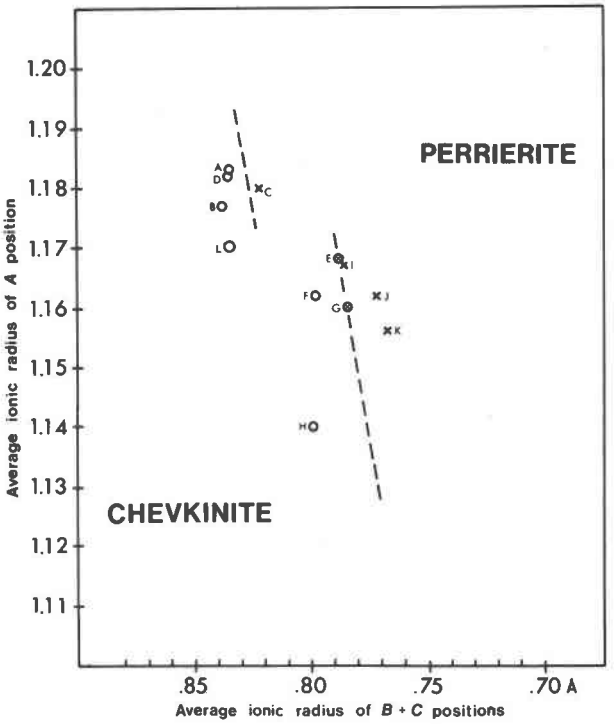

Fig. 4. Distribution of natural perrierites and chevkinites as a function of the average ionic radii of the *A* and *B* + *C* positions. Circles: chevkinites; crosses: perrierites; circled crosses: chevkinite → perrierite on heating in air. Plots A–D (Oslo region) this work, Table 2, Fe^{2+}/Fe^{3+} chosen as 3/1; plots E (Madagascar), G (Il'menskie Mts., U.S.S.R.), I (Italy) after Vlasov (1966); plots F (New Hampshire), H (Korea), J (Virginia), K (Japan) after Jaffe *et al.* (1956); plot L (Arizona) after Kauffman and Jaffe (1946).

to a 6-fold coordination (*B* or *C*) site. Ca in the eight previous analyses, except the Arizona chevkinite, occupied the *A* positions together with the REE. For our four points we have drawn a new phase boundary parallel to but not coincident with Ito's boundary. It is not unreasonable to assume that chemical differences could cause such a shift in the boundary between the perrierite and chevkinite fields. The shift is probably not due to a temperature effect, because Ito's experiments were conducted at 700°C and the Oslo region pegmatites are unlikely to have crystallized at temperatures much below this.

If one examines the chevkinite–perrierite structure as determined by Calvo and Faggiani (1974) one can explain the reason for the phase change. The main features of the chevkinite and perrierite structures are the same. Both consist of alternating layers (Fig. 5), in which one layer consists of *C* cations in octahedral coordination with oxygen and the other layer of $B(Si_2O_7)_2$ groups. Because the layers are firmly linked by shared oxygens, the size of the *B* and *C* cations exerts a strong control over the size of the unit cell. In the chevkinite structure very large cations can therefore only be accomodated in the *A* positions either by

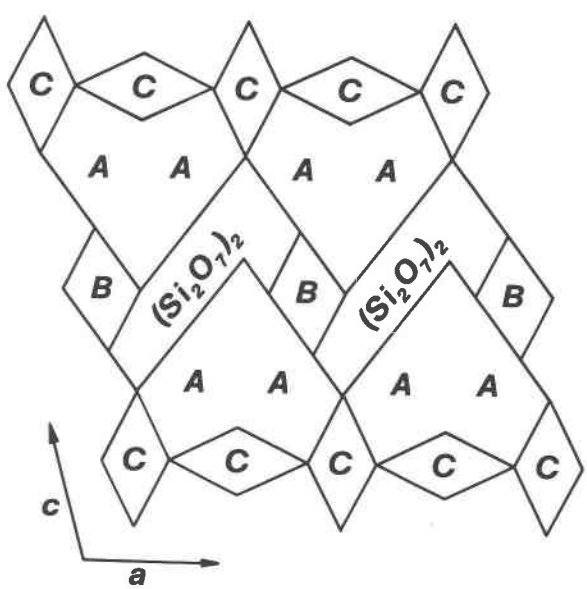

Fig. 5. Diagrammatic 010 projection of the chevkinite–perrierite structure according to Calvo and Faggiani (1974); a middle layer of $B(Si_2O_7)_2$ groups has octahedrally coordinated layers of *C* cations both above and below.

increasing the average size of the *B* and *C* cations to open up the structure or by distorting it to give it perrierite symmetry. In the latter case the Si_2O_7 groups are lengthened by increasing the Si–O–Si angle (157.4° in chevkinite and 165.6° in perrierite) and the octahedral layers are expanded by increasing the degree of distortion in the octahedron (the *C–C* distance is 2.863A in Nd/Mg chevkinite and 2.917A in La/Mg perrierite, the *C* position being occupied in both cases by Ti and Mg; Calvo and Faggiani, 1974).

Conclusion

The results of this study tend to confirm the conclusions of Ito (1967) and Ito and Arem (1971) that the phase change chevkinite–perrierite is controlled primarily by composition. It also indicates that the simple plot used by Ito has its limitations when dealing with the complex patterns of substitution encountered in naturally-occurring materials.

Acknowledgments

The authors are especially grateful to Brenda B. Jensen for substantial discussions and for her helpful comments on the first draft. The manuscript benefited from critical reviews by H. W. Jaffe, J. Ito, and C. Klein. Chevkinite samples from Sandefjord were kindly put to our disposal by Ragnar Hansen. The microprobe analyses were financed through grants to the first author from The Nansen Foundation and H. Bjørum's Legacy, which are gratefully acknowledged.

References

Albee, A. L. and L. Ray (1970) Correction factors for electron probe microanalysis of silicates, oxides, carbonates, phosphates, and sulfates. *Anal. Chem., 42,* 1408–1414.

Åmli, R. and W. L. Griffin (1975) Microprobe analysis of REE minerals using empirical correction factors. *Am. Mineral., 60,* 599–606.

Bence, A. E. and A. L. Albee (1968) Empirical correction factors for the electron microanalysis of silicates and oxides. *J. Geol., 76,* 382–403.

Bonatti, S. (1959) Chevkinite, perrierite and epidotes. *Am. Mineral., 44,* 115–137.

——— and G. Gottardi (1950) Perrierite, nuovo minerale ritrovato nella sabbia di Nettuno (Roma). *Acc. Naz. Lincei Rend. Sc. Fis. Mat. e Nat., 9,* 361–368.

——— and ——— (1966) Un caso di polimorfisma a strati in sorosilicati: perrierite e chevkinite. *Period. Mineral., 35,* 69–91.

Brøgger, W. C. (1890) Die Mineralien der Syenitpegmatitgänge der südnorwegischen Augit- und Nephelinsyenite. *Z. Krystallogr., 16,* 1–898.

Calvo, C. and R. Faggiani (1974) A re-investigation of the crystal structures of chevkinite and perrierite. *Am. Mineral., 59,* 1277–1285.

Gottardi, G. (1960) Crystal structure of perrierite. *Am. Mineral., 45,* 1–14.

Ito, J. (1967) A study of chevkinite and perrierite. *Am. Mineral., 52,* 1094–1104.

——— and J. E. Arem (1971) Chevkinite and perrierite: synthesis, crystal growth and polymorphism. *Am. Mineral., 56,* 307–319.

Izett, G. A. and R. E. Wilcox (1968) Perrierite, chevkinite, and allanite in upper Cenozoic ash beds in the western United States. *Am. Mineral., 53,* 1558–1567.

Jaffe, H. W., H. T. Evans, Jr. and R. W. Chapman (1956) Occurrence and age of chevkinite from the Devil's Slide fayalite-quartz syenite near Stark, New Hampshire. *Am. Mineral., 41,* 474–487.

Kauffman, A. J. and Jaffe, H. W. (1946) Chevkinite (tscheffkinite) from Arizona. *Am. Mineral., 31,* 582–588.

Lima-de-Faria, J. (1962) Heat treatment of chevkinite and perrierite. *Mineral. Mag., 33,* 42–47.

——— (1964) *Identification of Metamict Minerals by X-ray Powder Photographs.* Estud., Ensaios, Doc., Invest. Ultramar., Lisbon, Portugal.

Mitchell, R. S. (1966) Virginia metamict minerals: perrierite and chevkinite. *Am. Mineral., 51,* 1394–1405.

Portnov, A. M. (1964) Strontian perrierite in the northern Baikal region. (in Russian) *Dokl. Akad. Nauk. SSSR 156,* 579–581.

Raade, G. (1970) Contributions to the mineralogy of Norway, no. 43. Perrierite from the Sogndal anorthosite, south Norway. *Norsk Geol. Tidsskr., 50,* 241–243.

——— (1973) *Distribution of Radioactive Elements in the Plutonic Rocks of the Oslo Region.* Unpubl. thesis, University of Oslo.

Segalstad, T. V. and A. O. Larsen (1978) Gadolinite-(Ce) from Skien, southwestern Oslo region, Norway. *Am. Mineral., 63,* 188–195.

Shannon, R. D. and C. T. Prewitt (1969) Effective ionic radii in oxides and fluorides. *Acta Crystallogr., 25,* 925–946.

Vlasov, K. A., Ed. (1966) *Geochemistry and Mineralogy of Rare Elements and Genetic Types of their Deposits. II.* Israel Program for Scientific Translations, Jerusalem.

Manuscript received, August 29, 1977; accepted for publication, January 18, 1978.